



Slip rate determined from cosmogenic nuclides on normal-fault facets

Jim Tesson, Lucilla Benedetti, Vincent Godard, Catherine Novaes, Jules Fleury

► To cite this version:

Jim Tesson, Lucilla Benedetti, Vincent Godard, Catherine Novaes, Jules Fleury. Slip rate determined from cosmogenic nuclides on normal-fault facets. *Geology*, 2021, 49 (1), pp.66-70. 10.1130/G47644.1 . hal-03453637

HAL Id: hal-03453637

<https://hal.science/hal-03453637>

Submitted on 28 Nov 2021

HAL is a multi-disciplinary open access archive for the deposit and dissemination of scientific research documents, whether they are published or not. The documents may come from teaching and research institutions in France or abroad, or from public or private research centers.

L'archive ouverte pluridisciplinaire **HAL**, est destinée au dépôt et à la diffusion de documents scientifiques de niveau recherche, publiés ou non, émanant des établissements d'enseignement et de recherche français ou étrangers, des laboratoires publics ou privés.

Slip rate determined from cosmogenic nuclides on normal-fault facets.

Tracking no: G47644R

Authors:

Jim Tesson (CNRS), Lucilla Benedetti (CNRS), Vincent Godard (Aix-Marseille University), Catherine Novaes (CNRS), Jules Fleury (CNRS), and Team Aster (CNRS)

Abstract:

Facets are major topographic features built over several 100 kyrs above active normal faults. Their development integrates cumulative displacements over a longer timeframe than many other geomorphological markers and they are widespread in diverse extensional settings. We have determined the ^{36}Cl cosmogenic nuclide concentration on limestone faceted spurs at 4 sites in the Central Apennines, representing variable facet height (100-400 m). The ^{36}Cl concentration profiles show nearly constant values over the height of the facet suggesting the facet slope has reached a steady-state equilibrium for ^{36}Cl production. We model the ^{36}Cl build-up on a facet based on a gradual exposure of the sample resulting from fault slip and denudation. Data inversion with this forward model yields accurate constraints on fault slip-rates over the last 20-200 ka, which are in agreement with long-term rate independently determined on some of those faults over the last 1 Ma. ^{36}Cl measurements on faceted spurs can therefore constrain fault slip-rate over time spans that reach up to 200 ka, a time period presently under-sampled in most morpho-tectonic studies.

Slip rate determined from cosmogenic nuclides on normal-fault facets.

Jim Tesson¹, Lucilla Benedetti¹, Vincent Godard¹, Catherine Novaes¹, Jules Fleury¹ and ASTER Team^{1,1}

I-Aix Marseille Univ, CNRS, IRD, INRAE, Coll France, CEREGE, Aix-en-Provence, France

ABSTRACT

Facets are major topographic features built over several 100 kyrs above active normal faults. Their development integrates cumulative displacements over a longer timeframe than many other geomorphological markers and they are widespread in diverse extensional settings. We have determined the ^{36}Cl cosmogenic nuclide concentration on limestone faceted spurs at 4 sites in the Central Apennines, representing variable facet height (100-400 m). The ^{36}Cl concentration profiles show nearly constant values over the height of the facet suggesting the facet slope has reached a steady-state equilibrium for ^{36}Cl production. We model the ^{36}Cl build-up on a facet based on a gradual exposure of the sample resulting from fault slip and denudation. Data inversion with this forward model yields accurate constraints on fault slip-rates over the last 20-200 ka, which are in agreement with long-term rate independently determined on some of those faults over the last 1 Ma. ^{36}Cl measurements on faceted spurs can therefore constrain fault slip-rate over time spans that reach up to 200 ka, a time period presently under-sampled in most morpho-tectonic studies.

INTRODUCTION

Facets are characteristic landforms associated with the activity of normal faults (Wallace 1978, Armijo et al. 1986). But their potential as tectonic markers and the possibility of retrieving quantitative information on long-term slip rates from their morphological attributes and rates of evolution have seldom been considered (Petit et al. 2009, Tucker et al. 2011). This is an attractive prospect, as faceted spur development integrates cumulative displacements over a longer timeframe (100's of ka) than most other geomorphological markers and are ubiquitous in uplifting landscapes bounded by active normal faults. Quantifying tectonic deformation over Quaternary timescales usually relies on the analysis of passive morphological markers formed by various types of processes, such as fluvial or

¹*G. Aumaître, D.L. Boulès, K. Keddadouche*

30 marine terraces, moraines and landslides. In many settings the temporal record of such
31 markers spans only a few 10 ka, leaving the 100 ka timescale usually poorly documented
32 (Ryerson et al. 2006, Gold et al. 2016), which is a major hindrance for our understanding of
33 how deformation is accommodated. Triangular facets, on the other hand, are not passively
34 deformed markers but result from the combination of sustained rock uplift of the normal fault
35 footwall and its long-term erosion (Burbank and Anderson 2011).

36 Here, we provide the first systematic investigation of the use of the ^{36}Cl cosmogenic
37 nuclide to assess the rates of facet evolution. Our goal is to link cosmogenic nuclide buildup
38 on limestone faceted spurs and fault slip-rate by investigating 4 sites in the Central
39 Apennines, Italy of different shape and height (Fig 1). Following on Tucker et al. (2011)'s
40 assumptions linking facet slope, denudation rate and fault slip-rate, we compute the
41 theoretical ^{36}Cl concentration buildup of a facet as a function of its evolution with time (Fig.
42 2). The inversion of data acquired from the 4 studied sites demonstrates that our approach
43 provides accurate constraints on fault slip rates over time-spans ≤ 200 ka (Fig. 3 and 4).

44 **1- THEORETICAL ^{36}Cl BUILD UP ON A TRIANGULAR FACET**

46 Faceted spurs are near planar triangular or trapezoidal surfaces produced by the erosion of
47 normal fault scarps that are continuously rejuvenated at their base by sustained slip (Wallace
48 1978). Here we focus on normal fault footwalls formed in resistant bedrock and undergoing a
49 weathering-limited evolution (Tucker et al. 2011). Morphological evolution models (Tucker
50 et al. 2011, Strak et al. 2011, Tucker et al. 2020) suggest facet morphology reflects an
51 equilibrium between rock uplift from fault slip and erosion.

52 At the base of the facets, well-preserved bedrock fault scarps representing the cumulative
53 displacement on the fault since the last glacial maximum can be observed (Wallace 1978,
54 Armijo et al. 1992). This has been confirmed in the Mediterranean by exposure-age dating in
55 Greece, Italy, Israel, Turkey (e.g. Benedetti et al. 2013, Cowie et al. 2017). Post-glacial
56 changes in climatic conditions result in a decrease in hillslope erosion rates and preservation
57 of those bedrock fault scarps (Armijo et al. 1998, Allen et al. 1999). The timing of this shift is
58 not accurately dated and may spatially vary. In the Apennines, it is estimated to be 12-21 ka
59 (Giraudi 2017).

60 Based on these previous observations we use a two-stage kinematic model to predict ^{36}Cl
61 buildup in material currently exposed along the facet surface. First, under glacial conditions,
62 we assume topographic steady state, such that rock uplift of the footwall is equal to the

denudation rate of the facet surface. Rock sample are progressively exhumed parallel to the slip vector at a rate set by the fault slip-rate (Fig 2). Second, in post glacial conditions, we assume denudation of the facet to be negligible, such that rock samples are continuously exposed at the surface, with no significant regolith cover (Tucker et al., 2011).

Our approach relies on the interpretation of measured ^{36}Cl concentration at the surface in terms of this exhumation and exposure history of the facet. Based on the conceptual evolution described above, we parametrize this evolution using the time at which the sample starts moving towards the surface (T_{exhum}), the rate at which the sample moves parallel to fault motion prior to post-glacial conditions (SR), and the duration of post-glacial exposure assumed without erosion (T_{pg}). We combine this simple model with equations describing cosmogenic nuclides buildup to predict ^{36}Cl concentrations at the surface of the facet for any combination of the 3 parameters (T_{exhum} , T_{pg} , SR) defining the prescribed history (Suppl.).

2- ^{36}Cl CONCENTRATION PROFILES ON 4 FACETED SPURS IN CENTRAL APENNINES

We focus on 4 facets formed in limestones located along 3 active faults in central Apennines (Italy). Since late Pliocene-early Pleistocene, active normal faults accommodate the SW-NE extension in the area (Roberts and Michetti 2004). The Velino-Magnola fault is a major structure of the range (~30 km long, Fig. 1) with facets up to 300-800 m high, where we sampled two sites MA1 and MA3 along the northern and central part of the fault, respectively. The Roccapreturo fault is shorter (10 km), with lower facets (100-150 m), and was sampled at site AR in the center of the fault. The Bazzano fault is a small (3 km long) antithetic fault, with several facets reaching 100-150 m high, sampled in its southern section at site BAZ (Suppl.). The surface of the 4 sampled facets displays regular slope 30-35° (Fig 3). The surface of the facet is characterized by an alternance of bedrock outcrop, small bedrock protrusions (< 1m high), and patches of soil and screes less than a few cm thick. The facets are generally bounded by entrenched non-perennial streams that flow perpendicular to the fault's strike, which suggests recent incision that is contemporaneous with fault development. The slopes of the colluvial wedge surface ($\alpha \sim 25\text{-}30$) and of the facets ($\gamma \sim 30\text{-}35$) are similar across sites, the fault dips (β) from 40° at MA1, to 65° at BAZ (Suppl.).

The facets were sampled following an up-dip fault transect (Suppl.). We focused sampling on the lower part of the facet, where the surface appears less rugged, and near the facet center to avoid increased erosion by bounding gullies. Samples are 5-10 cm thick pieces of bedrock, taken on the top of protruding (> 0.5 m) bedrock surfaces, avoiding places that could have

been covered by regolith. Each sample was chemically prepared for ^{36}Cl measurements (Suppl.). At MA3 and ARC, the ^{36}Cl concentrations are roughly constant all along the facet (Fig. 3), except at the base where they increase by about 30%. At MA1 and BAZ, facets are lower and there are fewer points of measurements, but we observe a similar pattern at MA1 with constant values at the top, a slight decrease and an abrupt increase at the base of facet. There are only 3 data points at BAZ with decreasing concentrations toward the base. The ^{36}Cl concentrations along all studied facets are thus roughly constant suggesting that the denudation rate on those features is approximately constant. This observation is consistent with a facet development model that assumes a constant denudation rate. Moreover while it has been usually assumed that erosion would vary with facet height (Tucker et al. 2020 and references there in), our results suggest that, on the facet we studied, this is not the case.

3-FAULT SLIP-RATE FROM ^{36}Cl DATA INVERSION

To constrain the fault slip-rate we carried out a Bayesian inversion of the observed ^{36}Cl concentrations where the model parameters are the individual slip-rates of the faults (SR_{MA3} , SR_{MA1} , SR_{ARC} , SR_{BAZ}), and the post-glacial period duration (T_{PG}), assumed to be the same for the 4 sites (T_{exhum} is fixed a priori see suppl.). A complete description of the inversion procedure using the GW-MCMC algorithm (Goodman and Weare 2010), the corresponding parameters and the numerical code are provided in the Suppl. The inversion yielded mean slip-rates of 3.0 ± 1.2 mm/yr for MA3, 0.2 ± 0.02 mm/yr for MA1, 0.4 ± 0.3 mm/yr for ARC, and 0.06 ± 0.02 mm/yr for BAZ (Fig. 3 and 4). The mean post-glacial duration, common to all sites, is 18.7 ± 2 ka.

The modeled ^{36}Cl concentrations recover the average observed values at the scale of the facet, but do not account for the variability in ^{36}Cl concentrations observed in the lower part of the transects (Fig. 3).

4-DISCUSSION

Local controls on ^{36}Cl concentration

In most cases, for the upper part, the inversion reproduces the mean ^{36}Cl concentration. Overall, the discrepancy between observed and modeled concentrations is at most 0.5×10^5 at $^{36}\text{Cl}/\text{g}$ rock except for the points at the base of each site where observed concentrations are systematically higher by as much as 20% (except BAZ). The discrepancy for the upper part of the profile could be attributed to the stochastic dynamics of local processes such as temporary cover by a few cm of scree or abrupt removal of bedrock fragments that would lower the observed amount of ^{36}Cl with respect to the predictions of our model. A scree cover of 10 cm

would yield a 10% decrease in ^{36}Cl concentration and could account for a large fraction of the observed intra-site variability (Suppl.). On the contrary, simulations for MA3 show that a scree cover of less than 5-10 cm yields an increase in [^{36}Cl]. This is due to a relatively large slip-rate (3 mm/yr), and high natural chlorine content of some samples (>50 ppm) that maximize ^{36}Cl production at depth 0 to 100 cm (Schimmelpfennig et al. 2009). Another possibility that explains such a discrepancy could be that the facet slope might be locally steeper than the mean value used in the model. A difference of 10° could increase ^{36}Cl concentration by about 7% (Suppl.). At the base of the profile, where observed concentrations are systematically higher by as much as 20% (except BAZ), the observed systematic increase in ^{36}Cl concentration cannot be attributed to such short wavelength random variability in surface processes. This portion is at the intersection between the bedrock scarp and the facet slope, which is defined in the model by the altitude of the bedrock scarp top. There is a high uncertainty in the altitude of this point, usually affected by sliding scree that could explain the discrepancy. The shielding calculation might also underestimate the effect of secondary neutrons produced through colluvial material or bedrock (Masarik and Wieler 2003, Balco 2014). The colluvial density and the dip of the colluvial slope also affect the ^{36}Cl content at the base of the profile and could additionally account for this discrepancy (Suppl.).

Duration of exhumation versus post-glacial exposure

The value of 18.7 ± 2 ka obtained for the post-glacial duration is consistent with the timing of the most important glacial retreat in the Apennines estimated at about 21 ka from lake deposits records and morainic deposit (Giraudi 2017). It also corroborates the exposure ages from the top of the bedrock scarp at 11-15 ka at similar sites around the Apennines (Benedetti et al. 2013, Cowie et al. 2017). The amount of ^{36}Cl accumulated during the exhumation phase under glacial conditions is controlled primarily by fault slip rates and accounts for 9% of the total ^{36}Cl budget for MA3, 58% for MA1, 24% for ARC and 66% for BAZ. It means that at MA3, 95% of the measured ^{36}Cl has been accumulated over the last 20 ka, at the other sites this integration time is much longer, with durations of 185 ka, 47 ka and 210 ka at MA1, ARC and BAZ, respectively. Our approach thus allows determining slip-rates averaged over time scales that range from 20 to 210 ka. It is noteworthy that slower slip-rates are more tightly constrained because the ^{36}Cl buildup at depth outweigh the post-glacial ^{36}Cl production.

Slip-rate variability over time and relationships with facet morphology

Slip-rates derived from inversion for the four studied sites are between 3 and 0.06 mm/yr which is within the range of observations over the Holocene for similar faults in the Apennines (Benedetti et al. 2013, Cowie et al. 2017). Sites MA3 and MA1 are less than 5 km

apart and located on two segments of the Magnola fault (Suppl.). ^{36}Cl exposure dating of the bedrock scarp at each site yield Holocene-averaged slip rates of 1 to 1.5 mm/yr at MA3 and MA1 (Schlagenhauf et al. 2011), which is comparable with the result obtained at MA3 (3 ± 1.2 mm/yr over 20 ka). On the other hand, the slip-rate at MA1 (0.2 ± 0.02 mm/yr over 185 ka) is much lower than the one determined over the last ≈ 15 ka by Schlagenhauf et al. (2011). This discrepancy may be related to the difference in time-scale, suggesting that the slip on the fault has considerably accelerated over the last ≈ 15 ka. Slip-rate variability through time has already been reported for the few faults worldwide where multiple time-scales records are available (Perouse and Wernicke 2017, Friedrich et al. 2003). Studies on normal fault growth have shown that slip-rate can be highly variable over the fault length and over time (Manighetti et al. 2005). Our results confirm those observations and provide data to link incremental earthquake slip events and fault growth. The Bazzano fault (site BAZ) is an antithetic fault of the Paganica fault that ruptured during the 2009 L'Aquila earthquake. Several studies have allowed determining the Paganica slip-rate over a few thousand years to the Middle Pleistocene (Pucci et al. 2019). All converge toward a slip-rate of less than 0.4 mm/yr. The rate obtained for the antithetic Bazzano fault of 0.06 ± 0.02 mm/yr over the last 210 ka would thus account for about 15% of the Paganica synthetic fault slip, which appears realistic (Boncio et al. 2010). The slip-rate at site AR of 0.4 ± 0.3 mm/yr over the last 47 ka is similar to the rate previously estimated from Falcucci et al. (2015) of 0.2-0.3 mm/yr over the last 1 ± 0.2 Ma.

The slip-rates obtained for the four sites vary with the facet height, with the highest rate at MA3 where facet is 800 m-high (Schlagenhauf et al. 2011). This is in agreement with DePolo and Anderson (2000) who carried out a statistical analysis on normal faults located in the Basin and Range and observed a logarithmic relationship between the height of the facet and the vertical slip-rate of the fault (ranging from 0.001 to 2 mm/yr). Based on numerical modelling experiments, Petit et al. (2009) and Strak et al. (2011) also derived a linear relationship between facet height and throw rate in agreement with our results.

CONCLUSIONS

Our study presents the first systematic CRN measurements across facets developed above normal faults. We observe strikingly consistent signals with near constant ^{36}Cl concentrations over the height of the studied facets, which suggests the facets are close to a morphological steady state with a constant denudation during their development. Accordingly, we performed inverse modeling of the concentration profiles and inferred slip rates over the last 20-200 ka, the results of which are in agreement with long-term rate independently determined on some

of those faults over the last 1 Ma. The integration time span for ^{36}Cl accumulation over the facets is longer than the postglacial history of these landscapes, suggesting that such measurements could provide slip rates estimates over a time window that is usually undersampled in most tectonic geomorphology studies.

ACKNOWLEDGMENTS

This work has been partly funded by the LABEX OT MED. M. Rizza and B. Ourion are greatly acknowledged for their help and support in the field.

FIGURES CAPTIONS

Fig. 1 : A) Tectonic map of the Lazio-Abruzzo fault system (Schlagenhauf et al. 2011, Benedetti et al. 2013) with the faults (red line) bounding the sampled facets (yellow arrows) and site names (sites names were kept as in Schlagenhauf et al. 2010). B) Photography of the F-MA1 facet with location of samples and Holocene bedrock fault scarp at the base of the facets.

Fig. 2 : A-Modelled topographic profile of normal escarpment following Tucker et. al (2011) model resulting from exhumation of the footwall, with slope of the colluvial wedge surface α , dipping angle of fault-plane β , and γ slope of facet surface.

Fig. 3 : Measured (black dot) and modeled ^{36}Cl concentrations obtained from Bayesian inversion (grey pdf) of samples collected on the 4 facets (MA3, MA1, AR, BAZ) in Central Italy, as a function of sample altitude. Reduced chi-squared values are MA3=6.4; MA1=8.2; AR=5.2; BAZ=19.6.

Fig. 4 : Results from Bayesian inversion of ^{36}Cl data acquired on facet. Probability densities are plotted as function of slip-rate and post-glacial period duration (T_{pg}), with contour lines representing 10, 30, 50, 70, 90 % highest density interval. Pdf of posterior distribution is also shown for each SR and for T_{pg} .

REFERENCES CITED

- Allen, J. R. M. et al. Rapid environmental changes in southern Europe during the last glacial period. *Nature* 400, 740–743 (1999).
- Armijo, R., Tapponnier, P., Mercier, J. L., & Han, T. L. (1986). Quaternary extension in southern Tibet: Field observations and tectonic implications. *Journal of Geophysical Research: Solid Earth*, 91(B14), 13803-13872.

- Armijo, R., Lyon-Caen, H., & Papanastassiou, D. (1992). East-west extension and Holocene normal-fault scarps in the Hellenic arc. *Geology*, 20(6), 491-494.
- Balco, G. (2014). Simple computer code for estimating cosmic-ray shielding by oddly shaped objects. *Quaternary Geochronology*, 22, 175-182.
- Benedetti, L., Manighetti, I., Gaudemer, Y., Finkel, R., Malavieille, J., Pou, K., ... & Keddadouche, K. (2013). Earthquake synchrony and clustering on Fucino faults (Central Italy) as revealed from in situ ³⁶Cl exposure dating. *Journal of Geophysical Research: Solid Earth*, 118(9), 4948-4974.
- Boncio, P., Pizzi, A., Brozzetti, F., Pomposo, G., Lavecchia, G., Di Naccio, D., & Ferrarini, F. (2010). Coseismic ground deformation of the 6 April 2009 L'Aquila earthquake (central Italy, Mw6. 3). *Geophysical Research Letters*, 37(6).
- Burbank, D. W., & Anderson, R. S. (2011). *Tectonic geomorphology*. John Wiley & Sons.
- Cowie, P. A., Phillips, R. J., Roberts, G. P., McCaffrey, K., Zijerveld, L. J. J., Gregory, L. C., ... & Freeman, S. P. H. T. (2017). Orogen-scale uplift in the central Italian Apennines drives episodic behaviour of earthquake faults. *Scientific reports*, 7, 44858.
- DePolo, C. M., & Anderson, J. G. (2000). Estimating the slip rates of normal faults in the Great Basin, USA. *Basin Research*, 12(3-4), 227-240.
- Friedrich, A. M., Wernicke, B. P., Niemi, N. A., Bennett, R. A., & Davis, J. L. (2003). Comparison of geodetic and geologic data from the Wasatch region, Utah, and implications for the spectral character of Earth deformation at periods of 10 to 10 million years. *Journal of Geophysical Research: Solid Earth*, 108(B4).
- Giraudi, C., & Giaccio, B. (2017). Middle Pleistocene glaciations in the Apennines, Italy: new chronological data and preservation of the glacial record. *Geological Society, London, Special Publications*, 433(1), 161-178.

- Gold, R. D., Cowgill, E., Arrowsmith, J. R., & Friedrich, A. M. (2017). Pulsed strain release on the Altyn Tagh fault, northwest China. *Earth and Planetary Science Letters*, 459, 291-300.
- Goodman, J., & Weare, J. (2010). Ensemble samplers with affine invariance. *Communications in applied mathematics and computational science*, 5(1), 65-80.
- Mitchell, S. G., Matmon, A., Bierman, P. R., Enzel, Y., Caffee, M., & Rizzo, D. (2001). Displacement history of a limestone normal fault scarp, northern Israel, from cosmogenic ³⁶Cl. *Journal of Geophysical Research: Solid Earth*, 106(B3), 4247-4264.
- Masarik, J., & Wieler, R. (2003). Production rates of cosmogenic nuclides in boulders. *Earth and Planetary Science Letters*, 216(1-2), 201-208.
- Manighetti, I., Campillo, M., Sammis, C., Mai, P. M., & King, G. (2005). Evidence for self-similar, triangular slip distributions on earthquakes: Implications for earthquake and fault mechanics. *Journal of Geophysical Research: Solid Earth*, 110(B5).
- Petit, C., Gunnell, Y., Gonga-Saholiariliva, N., Meyer, B., & Séguinot, J. (2009b). Faceted spurs at normal fault scarps: Insights from numerical modeling. *Journal of Geophysical Research: Solid Earth*, 114(B5).
- Pérouse, E., & Wernicke, B. P. (2017). Spatiotemporal evolution of fault slip rates in deforming continents: The case of the Great Basin region, northern Basin and Range province. *Geosphere*, 13(1), 112-135.
- Pucci, S., Villani, F., Civico, R., Di Naccio, D., Porreca, M., Benedetti, L., ... & Pantosti, D. (2019). Complexity of the 2009 L'Aquila earthquake causative fault system (Abruzzi Apennines, Italy) and effects on the Middle Aterno Quaternary basin arrangement. *Quaternary Science Reviews*, 213, 30-66.
- Roberts, G. P., and A. M. Michetti (2004), Spatial and temporal variations in growth rates along active normal fault systems: an example from The Lazio–Abruzzo Apennines, central Italy, *J. Struct. Geol.*, 26(2), 339–376, doi:10.1016/S0191-8141(03)00103-2.

Roberts, G. P., Raithatha, B., Sileo, G., Pizzi, A., Pucci, S., Walker, J. F., ... & Guerrieri, L. (2010). Shallow subsurface structure of the 2009 April 6 M w 6.3 L'Aquila earthquake surface rupture at Paganica, investigated with ground-penetrating radar. *Geophysical Journal International*, 183(2), 774-790.

Ryerson, F.J., Tapponnier, P., Finkel, R.C., Mériaux, A.-S., Van der Woerd, J., Lasserre, C., Chevalier, M.-L., Xu, X., Li, H., and King, G.C.P., 2006, Applications of morphochronology to the active tectonics of Tibet, in Siame, L.L., Bourlès, D.L., and Brown, E.T., eds., Application of cosmogenic nuclides to the study of Earth surface processes: The practice and the potential: Geological Society of America Special Paper 415, p. 61–86, doi: 10.1130/2006.2415(05).

Schimmelpfennig, I., Benedetti, L., Finkel, R., Pik, R., Blard, P. H., Bourles, D., ... & Williams, A. (2009). Sources of in-situ ³⁶Cl in basaltic rocks. Implications for calibration of production rates. *Quaternary Geochronology*, 4(6), 441-461.

Schlagenhauf, A., Gaudemer, Y., Benedetti, L., Manighetti, I., Palumbo, L., Schimmelpfennig, I., ... & Pou, K. (2010). Using in situ Chlorine-36 cosmonuclide to recover past earthquake histories on limestone normal fault scarps: a reappraisal of methodology and interpretations. *Geophysical Journal International*, 182(1), 36-72.

Schlagenhauf, A., Manighetti, I., Benedetti, L., Gaudemer, Y., Finkel, R., Malavieille, J., & Pou, K. (2011). Earthquake supercycles in Central Italy, inferred from ³⁶Cl exposure dating. *Earth and Planetary Science Letters*, 307(3-4), 487-500.

Strak, V., Dominguez, S., Petit, C., Meyer, B., & Loget, N. (2011). Interaction between normal fault slip and erosion on relief evolution: Insights from experimental modelling. *Tectonophysics*, 513(1-4), 1-19.

Tucker, G. E., McCoy, S. W., Whittaker, A. C., Roberts, G. P., Lancaster, S. T., & Phillips, R. (2011). Geomorphic significance of postglacial bedrock scarps on normal-fault footwalls. *Journal of Geophysical Research: Earth Surface*, 116(F1).

328 Tucker, G. E., Hobley, D. E., McCoy, S. W., & Struble, W. T. Modeling the Shape and
329 Evolution of Normal-Fault Facets. *Journal of Geophysical Research: Earth Surface*,
330 e2019JF005305.

331

332 Wallace, R. E. (1978). Geometry and rates of change of fault-generated range fronts, north-
333 central Nevada. *J. Res. US Geol. Surv*, 6(5), 637-650.

334

Figure 1

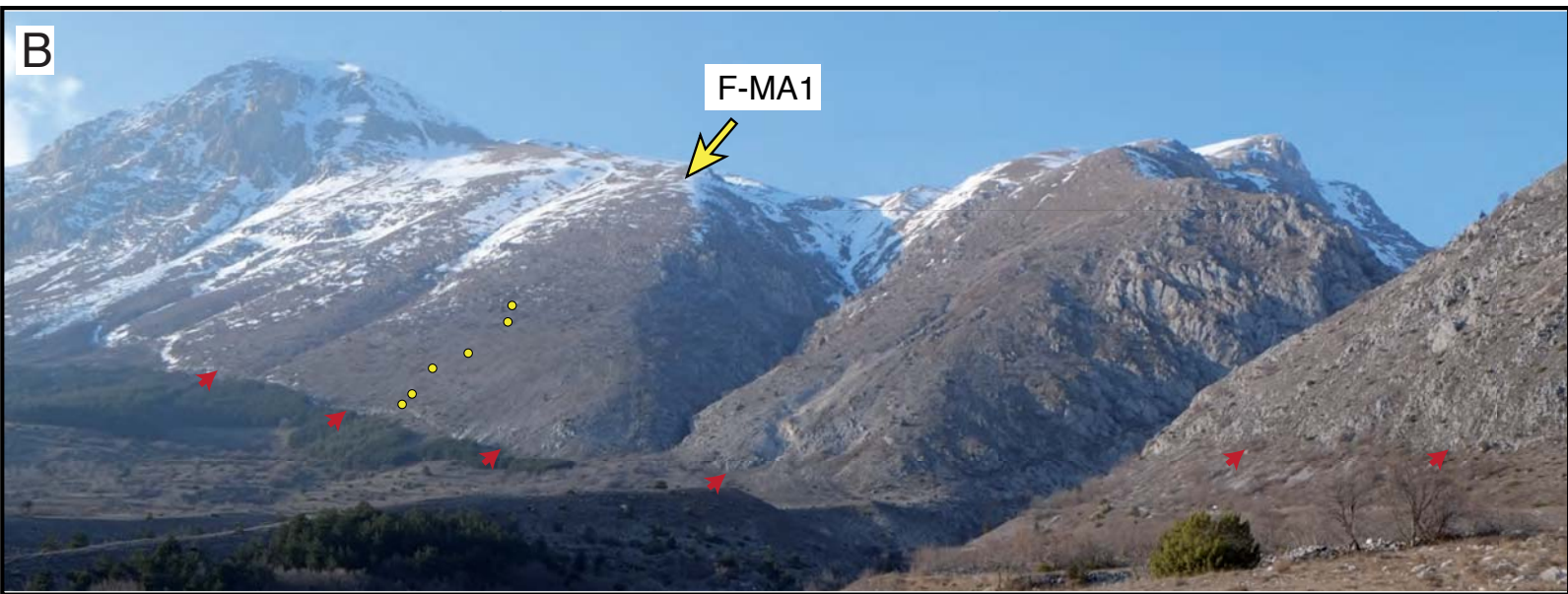
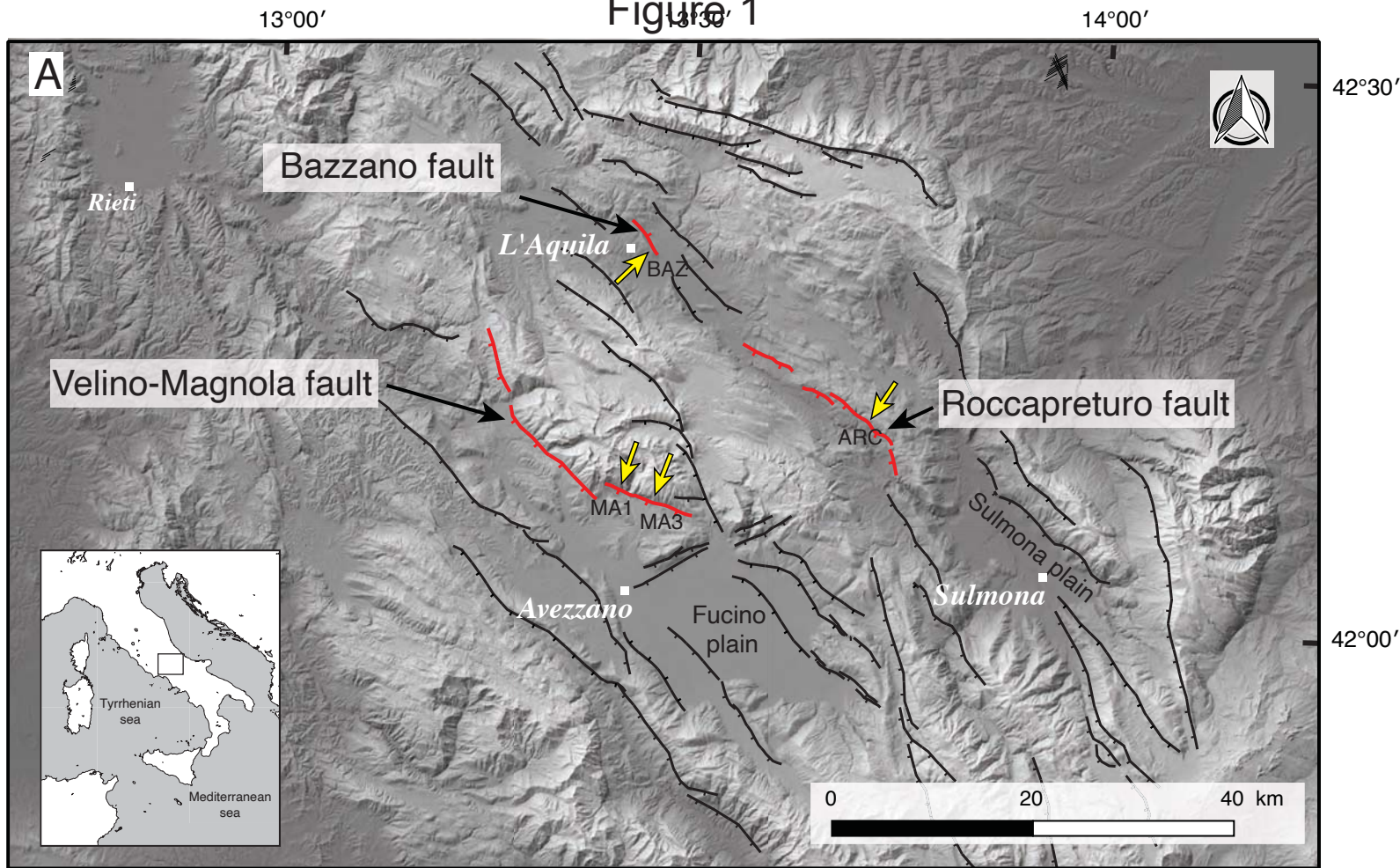


Figure 2

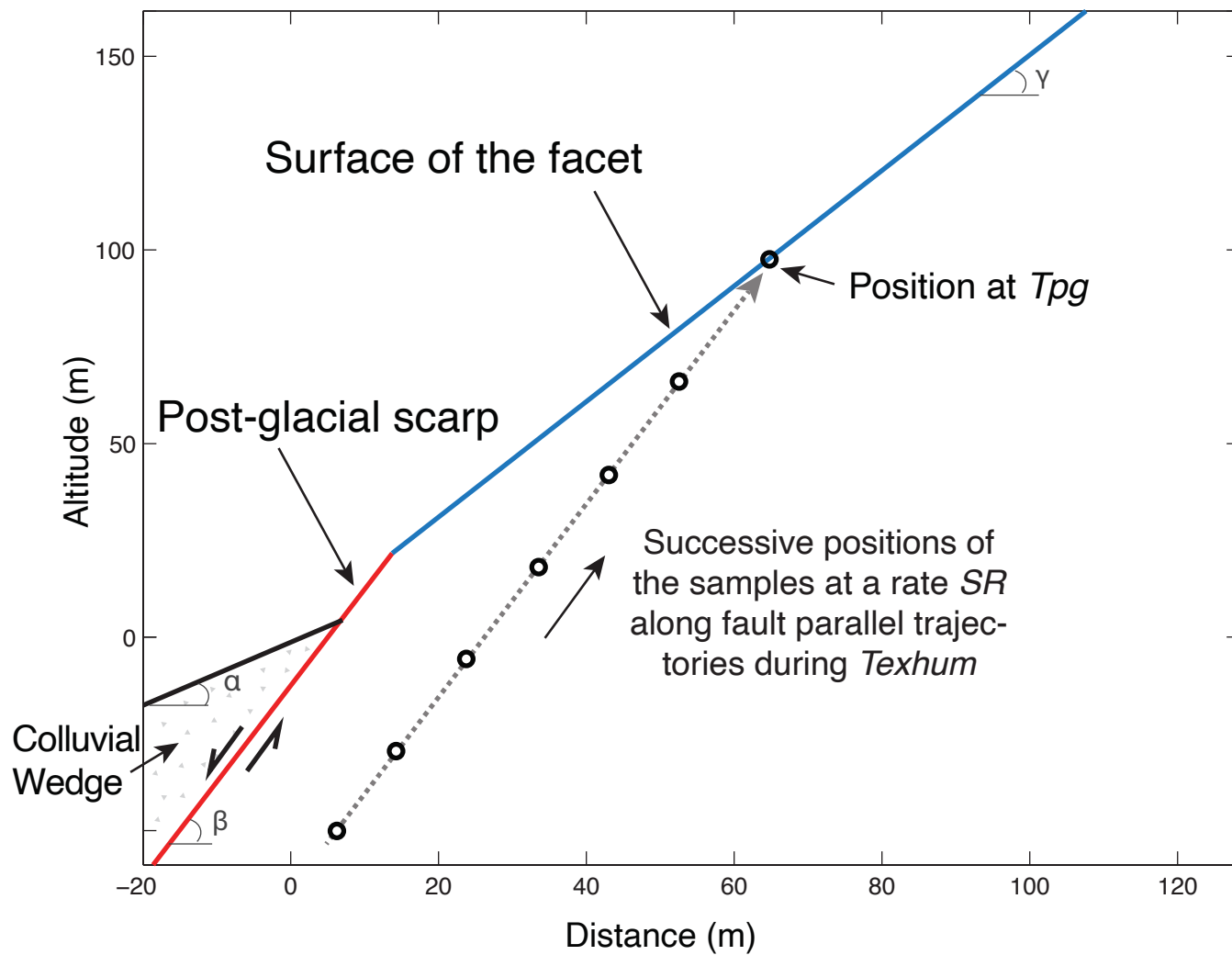


Figure 3

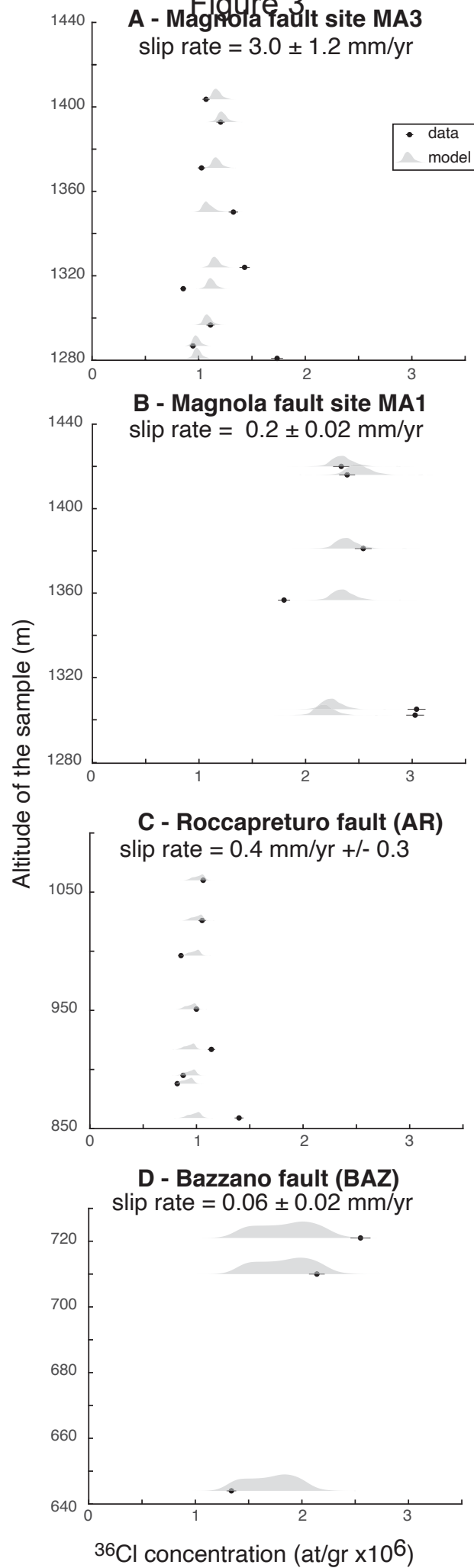
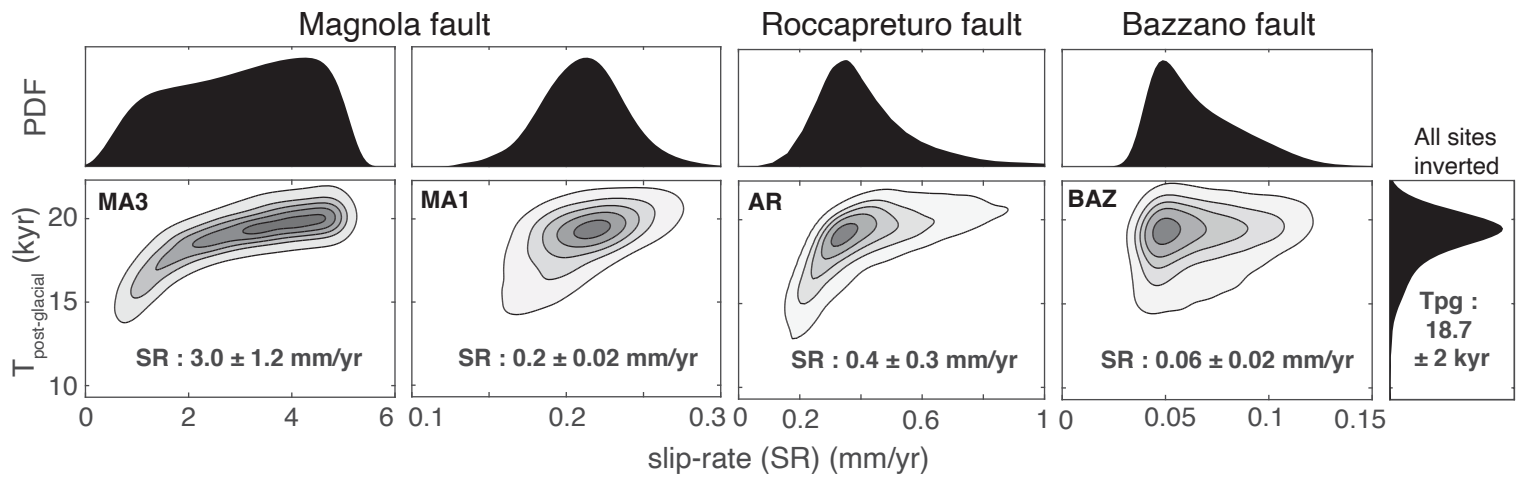


Figure 4



Slip rate determined from cosmogenic nuclides on normal-fault facets.

Jim Tesson¹, Lucilla Benedetti¹, Vincent Godard¹, Catherine Novaes¹, Jules Fleury¹ and ASTER Team^{1,1}

I-Aix Marseille Univ, CNRS, IRD, INRAE, Coll France, CEREGE, Aix-en-Provence, France

ABSTRACT

Facets are major topographic features built over several 100 kyrs above active normal faults. Their development integrates cumulative displacements over a longer timeframe than many other geomorphological markers and they are widespread in diverse extensional settings. We have determined the ^{36}Cl cosmogenic nuclide concentration on limestone faceted spurs at 4 sites in the Central Apennines, representing variable facet height (100-400 m). The ^{36}Cl concentration profiles show nearly constant values over the height of the facet suggesting the facet slope has reached a steady-state equilibrium for ^{36}Cl production. We model the ^{36}Cl build-up on a facet based on a gradual exposure of the sample resulting from fault slip and denudation. Data inversion with this forward model yields accurate constraints on fault slip-rates over the last 20-200 ka, **which** are in agreement with long-term rate independently determined on some of those faults over the last 1 Ma. ^{36}Cl measurements on faceted spurs can therefore constrain fault slip-rate over time spans that reach up to 200 ka, a time period presently under-sampled in most morpho-tectonic studies.

INTRODUCTION

Facets are characteristic landforms associated with the activity of normal faults (Wallace 1978, Armijo et al. 1986). But their potential as tectonic markers and the possibility of retrieving quantitative information on long-term slip rates from their morphological attributes and rates of evolution have seldom been considered (Petit et al. 2009, Tucker et al. 2011). This is an attractive prospect, as faceted spur development integrates cumulative displacements over a longer timeframe (100's of ka) than most other geomorphological markers and are ubiquitous in uplifting landscapes bounded by active normal faults. Quantifying tectonic deformation over Quaternary timescales usually relies on the analysis of passive morphological markers formed by various types of processes, such as fluvial or

¹*G. Aumâtre, D.L. Boulès, K. Keddadouche*

marine terraces, moraines and landslides. In many settings the temporal record of such markers spans only a few 10 ka, leaving the 100 ka timescale usually poorly documented (Ryerson et al. 2006, Gold et al. 2016), which is a major hindrance for our understanding of how deformation is accommodated. Triangular facets, on the other hand, are not passively deformed markers but result from the combination of sustained rock uplift of the normal fault footwall and its long-term erosion (Burbank and Anderson 2011).

Here, we provide the first systematic investigation of the use of the ^{36}Cl cosmogenic nuclide to assess the rates of facet evolution. Our goal is to link cosmogenic nuclide buildup on limestone faceted spurs and fault slip-rate by investigating 4 sites in the Central Apennines, Italy of different shape and height (Fig 1). Following on Tucker et al. (2011)'s assumptions linking facet slope, denudation rate and fault slip-rate, we compute the theoretical ^{36}Cl concentration buildup of a facet as a function of its evolution with time (Fig. 2). The inversion of data acquired from the 4 studied sites demonstrates that our approach provides accurate constraints on fault **slip rates over time-spans ≤ 200 ka** (Fig. 3 and 4).

1- THEORETICAL ^{36}Cl BUILD UP ON A TRIANGULAR FACET

Faceted spurs are near planar triangular or trapezoidal surfaces **produced by the erosion of normal fault scarps** that are continuously rejuvenated at their base by sustained slip (Wallace 1978). Here we focus on normal fault footwalls formed in resistant bedrock and undergoing a weathering-limited evolution (Tucker et al. 2011). Morphological evolution models (Tucker et al. 2011, Strak et al. 2011, Tucker et al. 2020) suggest facet morphology reflects an equilibrium **between rock uplift from fault slip and erosion**.

At the base of the facets, well-preserved bedrock fault scarps representing the cumulative displacement on the fault since the last glacial maximum can be observed (Wallace 1978, Armijo et al. 1992). This has been confirmed in the Mediterranean by exposure-age dating in Greece, Italy, Israel, Turkey (e.g. Benedetti et al. 2013, Cowie et al. 2017). **Post-glacial changes** in climatic conditions result in a decrease in hillslope erosion rates and preservation of those bedrock fault scarps (Armijo et al. 1998, Allen et al. 1999). The timing of this shift is not accurately dated and **may spatially vary**. In the Apennines, it is estimated to be 12-21 ka (Giraudi 2017).

Based on these previous observations we use a two-stage kinematic model to predict ^{36}Cl buildup in material currently exposed along the facet surface. First, under glacial conditions, **we assume topographic steady state, such that rock uplift of the footwall is equal to the**

denudation rate of the facet surface. Rock sample are progressively exhumed parallel to the slip vector at a rate set by the fault slip-rate (Fig 2). Second, in post glacial conditions, we assume denudation of the facet to be negligible, such that rock samples are continuously exposed at the surface, with no significant regolith cover (Tucker et al., 2011).

Our approach relies on the interpretation of measured ^{36}Cl concentration at the surface in terms of this exhumation and exposure history of the facet. Based on the conceptual evolution described above, we parametrize this evolution using the time at which the sample starts moving towards the surface (T_{exhum}), the rate at which the sample moves parallel to fault motion prior to post-glacial conditions (SR), and the duration of post-glacial exposure assumed without erosion (T_{pg}). We combine this simple model with equations describing cosmogenic nuclides buildup to predict ^{36}Cl concentrations at the surface of the facet for any combination of the 3 parameters (T_{exhum} , T_{pg} , SR) defining the prescribed history (Suppl.).

2- ^{36}Cl CONCENTRATION PROFILES ON 4 FACETED SPURS IN CENTRAL APENNINES

We focus on 4 facets formed in limestones located along 3 active faults in central Apennines (Italy). Since late Pliocene-early Pleistocene, active normal faults accommodate the SW-NE extension in the area (Roberts and Michetti 2004). The Velino-Magnola fault is a major structure of the range (~30 km long, Fig. 1) with facets up to 300-800 m high, where we sampled two sites MA1 and MA3 along the northern and central part of the fault, respectively. The Roccapreturo fault is shorter (10 km), with lower facets (100-150 m), and was sampled at site AR in the center of the fault. The Bazzano fault is a small (3 km long) antithetic fault, with several facets reaching 100-150 m high, sampled in its southern section at site BAZ (Suppl.). The surface of the 4 sampled facets displays regular slope 30-35° (Fig 3). The surface of the facet is characterized by an alternance of bedrock outcrop, small bedrock protrusions (< 1m high), and patches of soil and screes less than a few cm thick. The facets are generally bounded by entrenched non-perennial streams that flow perpendicular to the fault's strike, which suggests recent incision that is contemporaneous with fault development. The slopes of the colluvial wedge surface ($\alpha \sim 25\text{-}30$) and of the facets ($\gamma \sim 30\text{-}35$) are similar across sites, the fault dips (β) from 40° at MA1, to 65° at BAZ (Suppl.).

The facets were sampled following an up-dip fault transect (Suppl.). We focused sampling on the lower part of the facet, where the surface appears less rugged, and near the facet center to avoid increased erosion by bounding gullies. Samples are 5-10 cm thick pieces of bedrock, taken on the top of protruding (> 0.5 m) bedrock surfaces, avoiding places that could have

been covered by regolith. Each sample was chemically prepared for ^{36}Cl measurements (Suppl.). At MA3 and ARC, the ^{36}Cl concentrations are roughly constant all along the facet (Fig. 3), except at the base where they increase by about 30%. At MA1 and BAZ, facets are lower and there are fewer points of measurements, but we observe a similar pattern at MA1 with constant values at the top, a slight decrease and an abrupt increase at the base of facet. There are only 3 data points at BAZ with decreasing concentrations toward the base. The ^{36}Cl concentrations along all studied facets are thus roughly **constant** suggesting that the denudation rate on those features is approximately constant. This observation is consistent with a facet development model that **assumes a constant denudation rate**. Moreover while it has been usually assumed that erosion would vary with facet height (Tucker et al. 2020 and references there in), our results suggest that, on the facet we studied, this is not the case.

3-FAULT SLIP-RATE FROM ^{36}Cl DATA INVERSION

To constrain the fault slip-rate we carried out a Bayesian inversion of the observed ^{36}Cl concentrations where the model parameters are the individual slip-rates of the faults (SR_{MA3} , SR_{MA1} , SR_{ARC} , SR_{BAZ}), and the post-glacial period duration (T_{PG}), assumed to be the same for the 4 sites (T_{exhum} is fixed a priori see suppl.). A complete description of the inversion procedure using the GW-MCMC algorithm (Goodman and Weare 2010), the corresponding parameters and the numerical code are provided in the Suppl. The inversion yielded mean slip-rates of 3.0 ± 1.2 mm/yr for MA3, 0.2 ± 0.02 mm/yr for MA1, 0.4 ± 0.3 mm/yr for ARC, and 0.06 ± 0.02 mm/yr for BAZ (Fig. 3 and 4). The mean post-glacial duration, common to all sites, is 18.7 ± 2 ka.

The modeled ^{36}Cl concentrations **recover the average** observed values at the scale of the facet, but do not account for the variability in ^{36}Cl concentrations observed in the lower part of the transects (Fig. 3).

4-DISCUSSION

Local controls on ^{36}Cl concentration

In most cases, for the upper part, the inversion **reproduces the mean** ^{36}Cl concentration. Overall, the discrepancy between observed and modeled concentrations is at most 0.5×10^5 at $^{36}\text{Cl}/\text{g}$ rock except for the points at the base of each site where observed concentrations are systematically higher by as much as 20% (except BAZ). The discrepancy for the upper part of the profile could be attributed to the stochastic dynamics of local processes such as temporary cover by a few cm of scree or abrupt removal of bedrock fragments that would lower the observed amount of ^{36}Cl with respect to the predictions of our model. A scree cover of 10 cm

would yield a 10% decrease in ^{36}Cl concentration and could account for a large fraction of the observed intra-site variability (Suppl.). On the contrary, simulations for MA3 show that a scree cover of less than 5-10 cm yields an increase in [^{36}Cl]. This is due to a relatively large slip-rate (3 mm/yr), and high natural chlorine content of some samples (>50 ppm) that maximize ^{36}Cl production at depth 0 to 100 cm (Schimmelpfennig et al. 2009). Another possibility that explains such a discrepancy could be that the facet slope might be locally steeper than the mean value used in the model. A difference of 10° could increase ^{36}Cl concentration by about 7% (Suppl.). At the base of the profile, where observed concentrations are systematically higher by as much as 20% (except BAZ), the observed systematic increase in ^{36}Cl concentration cannot be attributed to such short wavelength random variability in surface processes. This portion is at the intersection between the bedrock scarp and the facet slope, which is defined in the model by the altitude of the bedrock scarp top. There is a high uncertainty in the altitude of this point, usually affected by sliding scree that could explain the discrepancy. The shielding calculation might also underestimate the effect of secondary neutrons produced through colluvial material or bedrock (Masarik and Wieler 2003, Balco 2014). The colluvial density and the dip of the colluvial slope also affect the ^{36}Cl content at the base of the profile and could additionally account for this discrepancy (Suppl.).

Duration of exhumation versus post-glacial exposure

The value of 18.7 ± 2 ka obtained for the post-glacial duration is consistent with the timing of the most important glacial retreat in the Apennines estimated at about 21 ka from lake deposits records and morainic deposit (Giraudi 2017). It also corroborates the exposure ages from the top of the bedrock scarp at 11-15 ka at similar sites around the Apennines (Benedetti et al. 2013, Cowie et al. 2017). The amount of ^{36}Cl accumulated during the exhumation phase under glacial conditions is controlled primarily by fault slip rates and accounts for 9% of the total ^{36}Cl budget for MA3, 58% for MA1, 24% for ARC and 66% for BAZ. It means that at MA3, 95% of the measured ^{36}Cl has been accumulated over the last 20 ka, at the other sites this integration time is much longer, with durations of 185 ka, 47 ka and 210 ka at MA1, ARC and BAZ, respectively. Our approach thus allows determining slip-rates averaged over time scales that range from 20 to 210 ka. It is noteworthy that slower slip-rates are more tightly constrained because the ^{36}Cl buildup at depth outweigh the post-glacial ^{36}Cl production.

Slip-rate variability over time and relationships with facet morphology

Slip-rates derived from inversion for the four studied sites are between 3 and 0.06 mm/yr which is within the range of observations over the Holocene for similar faults in the Apennines (Benedetti et al. 2013, Cowie et al. 2017). Sites MA3 and MA1 are less than 5 km

apart and located on two segments of the Magnola fault (Suppl.). ^{36}Cl exposure dating of the bedrock scarp at each site yield Holocene-averaged slip rates of 1 to 1.5 mm/yr at MA3 and MA1 (Schlagenhauf et al. 2011), which is comparable with the result obtained at MA3 (3 ± 1.2 mm/yr over 20 ka). On the other hand, the slip-rate at MA1 (0.2 ± 0.02 mm/yr over 185 ka) is much lower than the one determined over the last ≈ 15 ka by Schlagenhauf et al. (2011). This discrepancy may be related to the difference in time-scale, suggesting that the slip on the fault has considerably accelerated over the last ≈ 15 ka. Slip-rate variability through time has already been reported for the few faults worldwide where multiple time-scales records are available (Perouse and Wernicke 2017, Friedrich et al. 2003). Studies on normal fault growth have shown that slip-rate can be highly variable over the fault length and over time (Manighetti et al. 2005). Our results confirm those observations and provide data to link incremental earthquake slip events and fault growth. The Bazzano fault (site BAZ) is an antithetic fault of the Paganica fault that ruptured during the 2009 L'Aquila earthquake. Several studies have allowed determining the Paganica slip-rate over a few thousand years to the Middle Pleistocene (Pucci et al. 2019). All converge toward a slip-rate of less than 0.4 mm/yr. The rate obtained for the antithetic Bazzano fault of 0.06 ± 0.02 mm/yr over the last 210 ka would thus account for about 15% of the Paganica synthetic fault slip, which appears realistic (Boncio et al. 2010). The slip-rate at site AR of 0.4 ± 0.3 mm/yr over the last 47 ka is similar to the rate previously estimated from Falcucci et al. (2015) of 0.2-0.3 mm/yr over the last 1 ± 0.2 Ma.

The slip-rates obtained for the four sites vary with the facet height, with the highest rate at MA3 where facet is 800 m-high (Schlagenhauf et al. 2011). This is in agreement with DePolo and Anderson (2000) who carried out a statistical analysis on normal faults located in the Basin and Range and observed a logarithmic relationship between the height of the facet and the vertical slip-rate of the fault (ranging from 0.001 to 2 mm/yr). Based on numerical modelling experiments, Petit et al. (2009) and Strak et al. (2011) also derived a linear relationship between facet height and throw rate in agreement with our results.

CONCLUSIONS

Our study presents the first systematic CRN measurements across facets developed above normal faults. We observe strikingly consistent signals with near constant ^{36}Cl concentrations over the height of the studied facets, which suggests the facets are close to a morphological steady state with a constant denudation during their development. Accordingly, we performed inverse modeling of the concentration profiles and inferred slip rates over the last 20-200 ka, the results of which are in agreement with long-term rate independently determined on some

of those faults over the last 1 Ma. The integration time span for ^{36}Cl accumulation over the facets is longer than the postglacial history of these landscapes, suggesting that such measurements could provide slip rates estimates over a time window that is usually undersampled in most tectonic geomorphology studies.

ACKNOWLEDGMENTS

This work has been partly funded by the LABEX OT MED. M. Rizza and B. Ourion are greatly acknowledged for their help and support in the field.

FIGURES CAPTIONS

Fig. 1 : A) Tectonic map of the Lazio-Abruzzo fault system (Schlagenhauf et al. 2011, Benedetti et al. 2013) with the faults (red line) bounding the sampled facets (yellow arrows) and site names (sites names were kept as in Schlagenhauf et al. 2010). B) Photography of the F-MA1 facet with location of samples and Holocene bedrock fault scarp at the base of the facets.

Fig. 2 : A-Modelled topographic profile of normal escarpment following Tucker et. al (2011) model resulting from exhumation of the footwall, with slope of the colluvial wedge surface α , dipping angle of fault-plane β , and γ slope of facet surface.

Fig. 3 : Measured (black dot) and modeled ^{36}Cl concentrations obtained from Bayesian inversion (grey pdf) of samples collected on the 4 facets (MA3, MA1, AR, BAZ) in Central Italy, as a function of sample altitude. Reduced chi-squared values are MA3=6.4; MA1=8.2; AR=5.2; BAZ=19.6.

Fig. 4 : Results from Bayesian inversion of ^{36}Cl data acquired on facet. Probability densities are plotted as function of slip-rate and post-glacial period duration (T_{pg}), with contour lines representing 10, 30, 50, 70, 90 % highest density interval. Pdf of posterior distribution is also shown for each SR and for T_{pg} .

REFERENCES CITED

- Allen, J. R. M. et al. Rapid environmental changes in southern Europe during the last glacial period. *Nature* 400, 740–743 (1999).
- Armijo, R., Tapponnier, P., Mercier, J. L., & Han, T. L. (1986). Quaternary extension in southern Tibet: Field observations and tectonic implications. *Journal of Geophysical Research: Solid Earth*, 91(B14), 13803-13872.

- Armijo, R., Lyon-Caen, H., & Papanastassiou, D. (1992). East-west extension and Holocene normal-fault scarps in the Hellenic arc. *Geology*, 20(6), 491-494.
- Balco, G. (2014). Simple computer code for estimating cosmic-ray shielding by oddly shaped objects. *Quaternary Geochronology*, 22, 175-182.
- Benedetti, L., Manighetti, I., Gaudemer, Y., Finkel, R., Malavieille, J., Pou, K., ... & Keddadouche, K. (2013). Earthquake synchrony and clustering on Fucino faults (Central Italy) as revealed from in situ ³⁶Cl exposure dating. *Journal of Geophysical Research: Solid Earth*, 118(9), 4948-4974.
- Boncio, P., Pizzi, A., Brozzetti, F., Pomposo, G., Lavecchia, G., Di Naccio, D., & Ferrarini, F. (2010). Coseismic ground deformation of the 6 April 2009 L'Aquila earthquake (central Italy, Mw6. 3). *Geophysical Research Letters*, 37(6).
- Burbank, D. W., & Anderson, R. S. (2011). *Tectonic geomorphology*. John Wiley & Sons.
- Cowie, P. A., Phillips, R. J., Roberts, G. P., McCaffrey, K., Zijerveld, L. J. J., Gregory, L. C., ... & Freeman, S. P. H. T. (2017). Orogen-scale uplift in the central Italian Apennines drives episodic behaviour of earthquake faults. *Scientific reports*, 7, 44858.
- DePolo, C. M., & Anderson, J. G. (2000). Estimating the slip rates of normal faults in the Great Basin, USA. *Basin Research*, 12(3-4), 227-240.
- Friedrich, A. M., Wernicke, B. P., Niemi, N. A., Bennett, R. A., & Davis, J. L. (2003). Comparison of geodetic and geologic data from the Wasatch region, Utah, and implications for the spectral character of Earth deformation at periods of 10 to 10 million years. *Journal of Geophysical Research: Solid Earth*, 108(B4).
- Giraudi, C., & Giaccio, B. (2017). Middle Pleistocene glaciations in the Apennines, Italy: new chronological data and preservation of the glacial record. *Geological Society, London, Special Publications*, 433(1), 161-178.

- Gold, R. D., Cowgill, E., Arrowsmith, J. R., & Friedrich, A. M. (2017). Pulsed strain release on the Altyn Tagh fault, northwest China. *Earth and Planetary Science Letters*, 459, 291-300.
- Goodman, J., & Weare, J. (2010). Ensemble samplers with affine invariance. *Communications in applied mathematics and computational science*, 5(1), 65-80.
- Mitchell, S. G., Matmon, A., Bierman, P. R., Enzel, Y., Caffee, M., & Rizzo, D. (2001). Displacement history of a limestone normal fault scarp, northern Israel, from cosmogenic ^{36}Cl . *Journal of Geophysical Research: Solid Earth*, 106(B3), 4247-4264.
- Masarik, J., & Wieler, R. (2003). Production rates of cosmogenic nuclides in boulders. *Earth and Planetary Science Letters*, 216(1-2), 201-208.
- Manighetti, I., Campillo, M., Sammis, C., Mai, P. M., & King, G. (2005). Evidence for self-similar, triangular slip distributions on earthquakes: Implications for earthquake and fault mechanics. *Journal of Geophysical Research: Solid Earth*, 110(B5).
- Petit, C., Gunnell, Y., Gonga-Saholiariliva, N., Meyer, B., & Séguinot, J. (2009b). Faceted spurs at normal fault scarps: Insights from numerical modeling. *Journal of Geophysical Research: Solid Earth*, 114(B5).
- Pérouse, E., & Wernicke, B. P. (2017). Spatiotemporal evolution of fault slip rates in deforming continents: The case of the Great Basin region, northern Basin and Range province. *Geosphere*, 13(1), 112-135.
- Pucci, S., Villani, F., Civico, R., Di Naccio, D., Porreca, M., Benedetti, L., ... & Pantosti, D. (2019). Complexity of the 2009 L'Aquila earthquake causative fault system (Abruzzi Apennines, Italy) and effects on the Middle Aterno Quaternary basin arrangement. *Quaternary Science Reviews*, 213, 30-66.
- Roberts, G. P., and A. M. Michetti (2004), Spatial and temporal variations in growth rates along active normal fault systems: an example from The Lazio–Abruzzo Apennines, central Italy, *J. Struct. Geol.*, 26(2), 339–376, doi:10.1016/S0191-8141(03)00103-2.

Roberts, G. P., Raithatha, B., Sileo, G., Pizzi, A., Pucci, S., Walker, J. F., ... & Guerrieri, L. (2010). Shallow subsurface structure of the 2009 April 6 M w 6.3 L'Aquila earthquake surface rupture at Paganica, investigated with ground-penetrating radar. *Geophysical Journal International*, 183(2), 774-790.

Ryerson, F.J., Tapponnier, P., Finkel, R.C., Mériaux, A.-S., Van der Woerd, J., Lasserre, C., Chevalier, M.-L., Xu, X., Li, H., and King, G.C.P., 2006, Applications of morphochronology to the active tectonics of Tibet, in Siame, L.L., Bourlès, D.L., and Brown, E.T., eds., Application of cosmogenic nuclides to the study of Earth surface processes: The practice and the potential: Geological Society of America Special Paper 415, p. 61–86, doi: 10.1130/2006.2415(05).

Schimmelpfennig, I., Benedetti, L., Finkel, R., Pik, R., Blard, P. H., Bourles, D., ... & Williams, A. (2009). Sources of in-situ ³⁶Cl in basaltic rocks. Implications for calibration of production rates. *Quaternary Geochronology*, 4(6), 441-461.

Schlagenhauf, A., Gaudemer, Y., Benedetti, L., Manighetti, I., Palumbo, L., Schimmelpfennig, I., ... & Pou, K. (2010). Using in situ Chlorine-36 cosmonuclide to recover past earthquake histories on limestone normal fault scarps: a reappraisal of methodology and interpretations. *Geophysical Journal International*, 182(1), 36-72.

Schlagenhauf, A., Manighetti, I., Benedetti, L., Gaudemer, Y., Finkel, R., Malavieille, J., & Pou, K. (2011). Earthquake supercycles in Central Italy, inferred from ³⁶Cl exposure dating. *Earth and Planetary Science Letters*, 307(3-4), 487-500.

Strak, V., Dominguez, S., Petit, C., Meyer, B., & Loget, N. (2011). Interaction between normal fault slip and erosion on relief evolution: Insights from experimental modelling. *Tectonophysics*, 513(1-4), 1-19.

Tucker, G. E., McCoy, S. W., Whittaker, A. C., Roberts, G. P., Lancaster, S. T., & Phillips, R. (2011). Geomorphic significance of postglacial bedrock scarps on normal-fault footwalls. *Journal of Geophysical Research: Earth Surface*, 116(F1).

328 Tucker, G. E., Hobley, D. E., McCoy, S. W., & Struble, W. T. Modeling the Shape and
329 Evolution of Normal-Fault Facets. *Journal of Geophysical Research: Earth Surface*,
330 e2019JF005305.

331

332 Wallace, R. E. (1978). Geometry and rates of change of fault-generated range fronts, north-
333 central Nevada. *J. Res. US Geol. Surv*, 6(5), 637-650.

334